Studying Water Vapor in the Atmospheric Surface Layer

D. I. Cooper (dcooper@lanl.gov), C.-Y. J. Kao, J. R. Reisner, and J. A. Archuleta (EES-8)

Interactions between the Earth's surface and its atmosphere play a fundamental role in a variety of processes of interest to EES Division. The exchange of water between plant communities and the atmosphere, in particular, is an important component of the climate system, and to a large degree, this exchange controls the local recycling of precipitation. In addition to the more traditional measuring techniques and modeling studies that are used in EES, we are using an advanced remote sensing system, a scanning Raman lidar, to understand the role of evapotranspiration, the process by which plants exchange water with the atmosphere.

Lidar, the optical equivalent of radar, is used in a variety of atmospheric science applications; the Los Alamos Raman system is designed to measure water-vapor concentrations at short-to-medium distances. This discussion of the Raman lidar's application to evapotranspiration over the San Pedro River riparian area in southern Arizona is an introduction to the instrument's capabilities.

Figure 1. The Los Alamos Raman Lidar.

Instrument Description

The Los Alamos Raman water-vapor lidar is based on the Raman technique pioneered in the 1960s and extended for daytime, solar-blind operation in the 1980s. In Figure 1 we see a photograph of the Los Alamos Raman lidar being set up for operation in Arizona. The device operates by emitting a pulsed, ultraviolet laser beam. The laser light is absorbed by nitrogen and water vapor molecules and re-emitted in their Raman bands. The lidar system then collects this "Raman-scattered" light and converts it to an electrical signal. The system operates in the solar-blind region of the spectrum using krypton fluoride as the lazing medium to obtain light at 248 nm. The Raman-shifted nitrogen signal returns at 263 nm, and the Raman-shifted water vapor signal returns at 273 nm. Simultaneous measurement of the water-vapor and nitrogen signal returns provides a simple method for obtaining absolute measurements.

Because nitrogen is by far the most abundant atmospheric gas and because its concentration is relatively invariant, dividing the Raman-shifted return signal from water vapor by that of nitrogen normalizes each pulse and corrects for first-order atmospheric transmission effects, pulse-to-pulse laser variations, and telescope field-of-view overlap with the laser beam. The normalized returns are then proportional to the absolute water-vapor content of the air. A correction is required to account for the differential atmospheric attenuation between the nitrogen and water-vapor wavelengths.

The typical maximum horizontal range for the lidar is approximately 700 m when scanning, with a corresponding spatial resolution of 1.5 m over that distance. The upper scanning mirror allows three-dimensional scanning in 360° in azimuth and ±22° in elevation. The uncertainty in the water-vapor mixing ratio is typically measured to be less than 4%.

Spatial Variations of Water Vapor

Here we present selected lidar-data analyses as vertical lidar scans of water-vapor concentration (in the form of mixing ratio) and as vertical profiles of water vapor derived from

the scans. The vertical scans represent vertical/horizontal cross-sections of the structure of atmospheric water vapor. Our analysis focuses on measurements over a cottonwood canopy versus measurements over the adjacent grass-shrub cover.

Water Vapor over a Canopy. In 1997, the Los Alamos Raman lidar system was fielded as a part of the Semi-Arid Land-Surface Atmosphere Experiment (SALSA) for the San Pedro Project in Arizona. The site chosen for this field study included both grassland/scrub areas and the cottonwood-bosque riparian area adjacent to the San Pedro River.

A cursory inspection of some of the lidar data obtained reveals interesting properties of the cottonwood-canopy/surface-layer interface, when compared with the atmosphere above the relatively flat grass-mesquite-sacaton region adjacent to the San Pedro riparian corridor. An example of a time series of vertical scans acquired between 0913 local standard time (LST) and 1436 LST on August 11, 1997, illustrates the spatial patterns and distribution of water vapor mixing ratio in 1.5-m, range-resolved pixels. The variations in color in the images of Figure 2 show high mixing-ratio values in red and low values in blue. The vertical scans are composed of 42 individual scan lines in which each scan required 0.75 s. Thus, it took about 32 s to complete and save each image. The lidar return signal from the cottonwood trees was substantially larger than the atmospheric signal and saturated the detectors; therefore, the returned signal from the leaves, stems, and trunks can be separated from the atmospheric signal by using a simple threshold. By setting all mixing-ratio values above 16.8 g/kg^{-1} as canopy signal and all values below 16.8 g/kg^{-1} as "atmospheric" signal, the canopy appears as solid red in the Figure 2 images.

The black regions on the images are areas for which the water vapor mixing ratio is below 10.5 g/kg^{-1}, the reading associated with the bottom-most color on the legend. When the return signal is less than 14.0 g/kg^{-1}, patterns emerge from the data, as can be seen in the unstable regions above the surface and the canopy.

Microscale convective structures above the canopy are seen as "bubbles" of high-mixing-ratio air presumably interacting with the relatively drier air from above, such as the structure at 430 m range and starting at 30 m height in the 0913 LST scan. At the time of this measurement, the wind was nearly perpendicular to the lidar line of sight. Over a green ash orchard, the lidar observed similar convective structures that were closely related to intermittent features, including "ramps." The high-mixing-ratio features over the mesquite-sacaton area are 2 to 3 g/kg^{-1} drier than those over the cottonwood canopy. Interestingly, these features appear primarily in the morning and decrease in frequency until they disappear at midday; after about 1330 hours LST, they begin reappearing. We still do not know if these structures are due to dynamics above the canopy or to canopy-atmosphere interactions such as sweep-ejection phenomena.

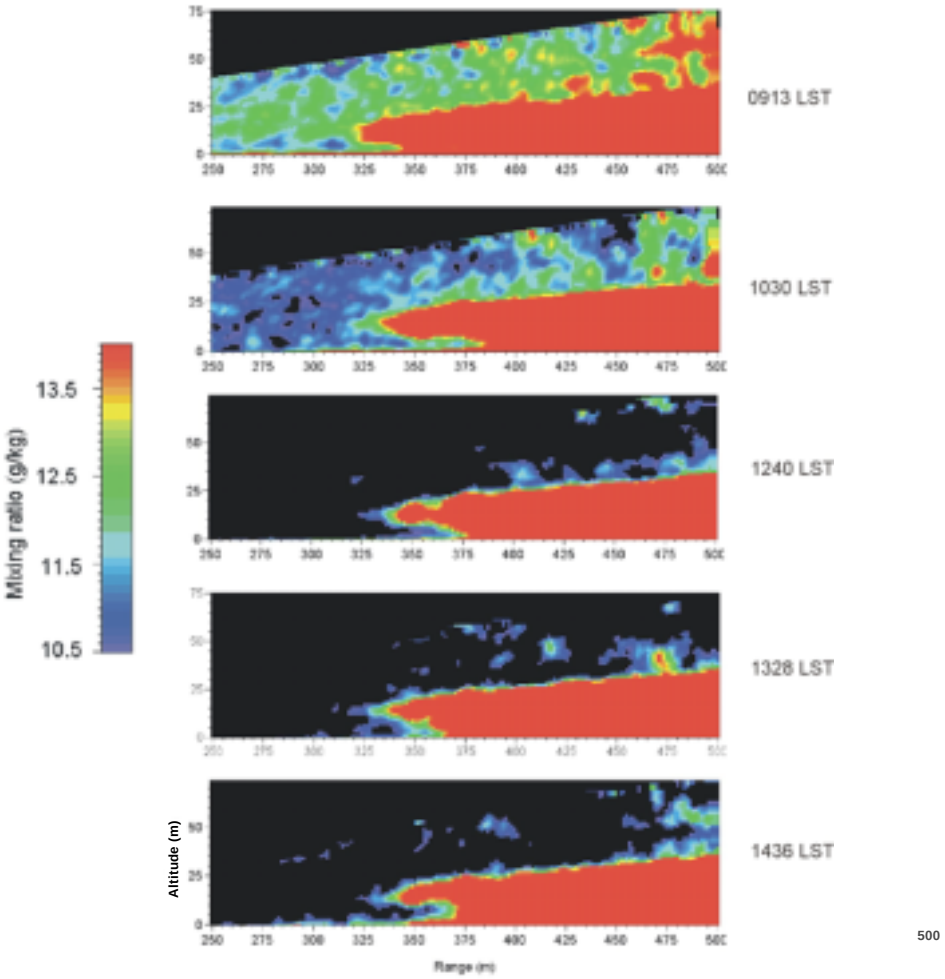

Figure 2. Lidar Scans over Cottonwoods and Grassland.
These scans show vertical cross sections of water vapor above the San Pedro River cottonwood bosque for a series of times indicated as local standard time (LST).

A more traditional method for displaying and analyzing the lidar data would be in the form of vertical profiles of water vapor extracted from the scans. We made one-dimensional profiles with 32-s averaging times by sorting the range pixels by their associated height bins from an individual scan shown in the Figure 2 cross sections. Thus, all range pixels from a given region that fell into a specified height range (e.g., from 0 to 0.5 m in elevation) can be displayed as mixing ratio versus height. We extracted two 25-m-wide sections from the 0913 LST scan in Figure 2 at positions over both the grass-mesquite-sacaton association (at ranges between 300 and 325 m) and the cottonwoods (between 425 and 450 m). The grass was in the near field of the scan, limiting the height of the profile to 35 m. The sixteen 1.5-m lidar values per height bin in these 25-m scan widths provide the data points of the profiles in Figure 3. Although the average mixing ratio is similar for the two regimes, there is a substantially larger variability at a given height over the cottonwoods. Both regimes exhibited an undulating structure with height, reflecting some of the coherent structures visible in the image in Figure 2. Figure 3 suggests that over both regimes the size of these structures is similar, approximately 20 m. The plumes observed in Figure 2 create the moistening observed 10 to 15 m above the canopy in the profiles of Figure 3; as these plumes decay in height, the profiles show these higher regions as "dry."

The most pronounced difference between the two profiles in Figure 3 is the variability of function of height above the canopy. While the mean mixing ratios for the grass and cottonwoods are only about 0.5 g/kg^{-1} apart, the range of values at a given height is approximately 2.5 times greater for the cottonwoods than for the grass. This difference shows that water vapor from the cottonwood provides greater atmospheric input than does water vapor from the grassland.

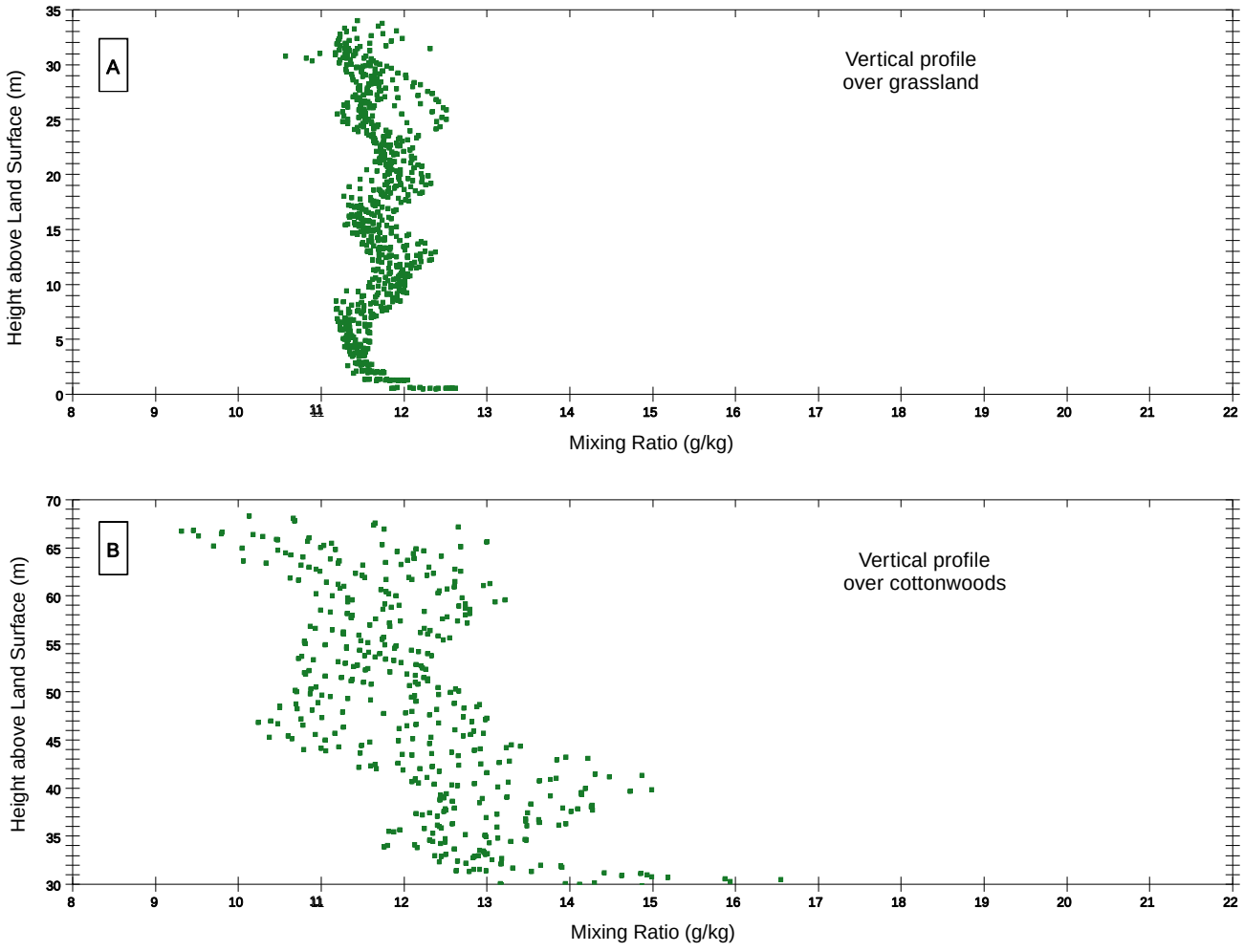

Figure 3. One-Dimensional Water-Vapor Profiles.
These vertical profiles from Figure 2 are of (A) water-vapor mixing ratio over grassland between the surface and to a height of about 35 m from the leftmost part of the Figure 2 images and (B) the ratio over cottonwoods between the tree tops and about 70 m.

Closing Comments

Understanding mixing processes in the atmospheric boundary layer and how they are influenced by—and influence—surface/atmosphere exchange processes is critical to understanding the Earth's hydrological and carbon cycles and the climate itself. Although numerical models provide great insight into these mixing processes, direct observations add a new dimension to our studies. The Los Alamos Raman lidar system can directly measure small-scale variations in atmospheric water vapor. Those variations are closely tied to the mechanisms of atmospheric mixing.

As shown by the example presented here, water vapor in the lower atmosphere is influenced strongly by the character of the Earth's surface itself, in this case by the differences between cottonwood canopies and grasslands. The greater evapotranspiration rates from the canopy in the SALSA experiment are reflected by higher water-vapor mixing ratios above the canopy. In addition, the scales of the mixing processes are shown by the sizes of the bubbles of high-mixing-ratio air and by the bubbles' progression in time.

We are conducting additional field studies using the Raman system. For example, we are participating in the DOE-funded vertical transport and mixing experiment, in which nocturnal mixing processes in the atmosphere above Salt Lake City are being studied. We are also conducting a variety of observational campaigns to promote understanding of evapotranspiration processes from various types of ground cover. These sets of measurements will address questions about the efficiency of water retention of various biomes, the differences between daytime and nighttime mixing processes (and the behavior of the transition between the two regimes), and the effects of these mixing processes on the transport and fate of atmospheric pollution. ■

Further Reading

Cooper, D. I., W. E. Eichinger, D. E. Hof, D. Seville-Jones, R. C. Quick, and J. Tiee. 1994. Observations of coherent structures from a scanning LIDAR over an irrigated orchard. *Agricultural and Forest Meteorology* **67**: 239–252.

Cooper, D. I., W. E. Eichinger, J. Kao, L. Hipps, J. Reisner, S. Smith, S. M. Schaeffer, and D. G. Williams. 2000. Spatial and temporal properties of water vapor and latent energy flux over a riparian canopy. *Agricultural and Forest Meteorology* **105**: 161–183.

Cooney, J., K. Petrik, and A. Salik. 1985. Measurement of high-resolution atmospheric water vapor profiles by use of a solar-blind, raman LIDAR. *Applied Optics* **24**: 104–108.

Eichinger, W., et al. 1992. Derivation of water vapor fluxes from LIDAR measurements. *Boundary-Layer Meteorology* **63**: 39.

Kao, C.-Y. J., Y. H. Hang, D. I. Cooper, W. E. Eichinger, W. S. Smith, and J. M. Reisner. 2000. High-resolution modeling of LIDAR data: Mechanisms governing surface water vapor variability during SALSA. *Agricultural and Forest Meteorology* **105**: 185–194.

Melfi, S. H., et al. 1969. Observation of raman scattering by water vapor in the atmosphere. *Applied Physics Letters* **15**: 295.